

The University of Bradford Institutional Repository

<http://bradscholars.brad.ac.uk>

This work is made available online in accordance with publisher policies. Please refer to the repository record for this item and our Policy Document available from the repository home page for further information.

To see the final version of this work please visit the publisher's website. Access to the published online version may require a subscription.

Link to publisher's version: <http://dx.doi.org/doi:10.1016/j.fuproc.2016.04.018>

Citation: Parvez AM, Mujtaba Iqbal M, Pang C, Lester E and Wu T (2016) Effect of the addition of different waste carbonaceous materials on coal gasification in CO₂ atmosphere. Fuel Processing Technology. 149: 231-238.

Copyright statement: © 2016 Elsevier B.V. Reproduced in accordance with the publisher's self-archiving policy. This manuscript version is made available under the [CC-BY-NC-ND 4.0 license](#)



Effect of the addition of different waste carbonaceous materials on coal gasification in CO₂ atmosphere

Ashak M. Parvez ^a, Iqbal M. Mujtaba ^b, Chengheng Pang ^a, Tao Wu ^{a,*}

^a Department of Chemical and Environmental Engineering, The University of Nottingham Ningbo China, Ningbo 315100, China

^b Chemical Engineering Division, School of Engineering, University of Bradford, Bradford BD7 1DP, UK

Corresponding author: Tao.Wu@nottingham.edu.cn

Abstract

In order to assess the utilisation of waste carbonaceous materials and the feasibility of using CO₂ as a gasifying agent, the gasification characteristics of coal, a suite of waste carbonaceous materials, and their blends were investigated by using a thermogravimetric analyser (TGA). The results showed that the CO₂ gasification process of polystyrene completed at 470 °C which was lower than other carbonaceous materials. This behaviour was attributed due to the high content of volatile coupled with its unique thermal degradation properties. It is found that the initial decomposition temperature decreased with the increasing amount of waste carbonaceous materials in the blends. Overall, CO₂ co-gasification process was enhanced as a direct consequence of interactions whose intensity and temperature of occurrence were influenced by the chemical and compositional properties of carbonaceous materials. The strongest interactions were noticed in coal/polystyrene blend at the devolatilisation stage as indicated by its highest value of Root Mean Square Interaction Index (RMSII), caused by highly reactive characteristic of polystyrene. On the other hand, coal/oat straw blend revealed the highest interactions at char gasification stage. The catalytic effect of alkali metals content in oat straw, particularly CaO and K₂O, was believed to be the reasons

23 for these strong interactions. Furthermore, co-pyrolysis was compared with CO₂ gasification
24 through RMSII value, while the effect of CO₂ as a gasifying agent on interactions during co-
25 gasification was also evaluated. It is clear from this study that CO₂ gasification of coal can be
26 enhanced significantly via the addition of polystyrene and oat straw.

27 **Keywords:** CO₂ gasification; Carbonaceous materials; Interactions; Catalytic effect

28 **1 Introduction**

29 In order to minimise CO₂ emissions, different waste carbonaceous materials are used as
30 energy source because of their carbon neutral nature. In recent years, co-utilisation of waste
31 carbonaceous materials has become increasingly popular to replace a portion of coal in
32 existing coal-fired boilers for power generation [1, 2].

33 Over the years, many techniques have been developed to utilise coal with biomass and other
34 carbonaceous materials. Co-gasification is one of the promising methods because it has the
35 potential to improve the gas yield and corresponding heating value of the product when low
36 quality coal is gasified [3, 4]. Moreover, improved overall carbon conversion and cold gas
37 efficiency can also be achieved by increasing the proportion of biomass in the feed.

38 For gasification process, CO₂ is a potential gasification medium [5-7]. It is less corrosive than
39 steam and can be used to adjust syngas composition for different applications [8]. In the past
40 decades, a lot of research has been carried out on biomass gasification using CO₂ as a

41 gasifying agent [5, 7, 9-12]. These researches were mainly focused on the kinetics [5, 9, 11,
42 12], gasification reactivity [7, 10, 13, 14] and gasification characteristics [14-16] in general.
43 In spite of huge potential of CO₂ in coal and biomass gasification, limited effort have been
44 made to understand gasification behaviours, particularly on interactions during co-gasification.
45 Apart from these, limited study has been conducted understanding how to enhance co-
46 gasification via choosing suitable waste carbonaceous materials for the co-gasification of
47 certain coal. In addition, information on waste carbonaceous materials such as non-metallic
48 part of printed circuit boards, tyre scraps and polystyrene are very limited compared with the
49 conventional fuel and biomass. Moreover, not much work has been performed to understand
50 the effects of CO₂ on the gasification process of these carbonaceous materials. Thus, there are
51 still needs to achieve in depth understanding of gasification characteristics of coal, waste
52 carbonaceous materials and their blends.

53 In this paper, gasification characteristics of coal, a suite of waste carbonaceous materials and
54 their blends were investigated in a TGA using CO₂ as the only gasifying agent. In addition,
55 the influence of mass fractions of carbonaceous materials on gasification characteristics of the
56 blends was analysed. The interactions during co-gasification were also studied and the reasons
57 for these interactions were explored.

58 **2 Experimental**

59 **2.1 Samples preparation**

60 In this study, an Australian bituminous coal was selected as the coal sample. Oat straw (OS),
61 Non-metallic part of printed circuit boards (NMPCBs), tyre scraps (tyre) and polystyrene (PS)
62 were chosen as the waste carbonaceous materials samples. All samples were air-dried at
63 ambient temperature prior to further processing. Size reduction was carried out by using an
64 industrial hammer crusher (CSF570, Fengli Pulverization Ltd., China) and ball mill (SM2000,
65 MM400, Retsch, Germany), respectively. All samples were ground to a size smaller than 106
66 microns (Endecott 106 microns aperture sieve) following the standard milling procedure
67 (CEN/TS 15443:2006). Before characterization and testing, all samples were treated
68 following international accepted standard procedure to ensure representativeness of the
69 samples [17]. The blend samples were prepared from these materials by mixing manually at
70 (coal to waste carbonaceous material) mass ratios of 90:10 and 70:30 (with a maximum
71 deviation of ± 0.1 mg), which is denoted as high and low blending ratios, respectively. These
72 ratios are representative of typical co-gasification parameters, corresponding to 5%-35% on
73 thermal basis.

74 **2.2 Sample characterisation**

75 Proximate analysis of the samples was conducted based on the standard practice for
76 Proximate Analysis using a TGA following procedures described elsewhere [18]. All the

77 experiments were repeated three times and average value was used for the study. Carbon (C),
78 hydrogen (H), nitrogen (N) and sulphur (S) contents were determined using a CHNS/O
79 Element Analyser (PE2400, PerkinElmer, USA) following the standard testing procedure
80 described in the manual. The standard sample was firstly applied to calibrate the Elemental
81 Analyser. Approximately 1.5 mg of dried fine powder was used for each test, which was
82 repeated at least three times. Oxygen content was calculated by difference on dry and ash free
83 basis. The tests were carried out in helium carrier gas with an accuracy of $\leq 0.3\%$ and a
84 precision of $\leq 0.2\%$. Calorific value of all the samples was determined using a calorimeter
85 (IKA C 200, Germany), which was calibrated prior to testing using benzoic acid to achieve a
86 relative standard deviation less than 0.2%. As for ash composition, each sample was analysed
87 twice using an X-Ray Diffraction (XRD) (Bruker D8 Advance, Germany) to minimize
88 experimental error to be within $\pm 1.5\%$.

89 **2.3 CO₂ gasification**

90 CO₂ gasification of the coal, waste carbonaceous materials and their blends was carried out
91 using a STA 449/F3 Jupiter thermal analyser (NETZSCH Geraetebau GmbH, Germany) with
92 a weighing precision of $\pm 0.01\%$ and TGA resolution of 0.1 μg . In each test, the sample was
93 heated to 50 °C in N₂ (30 ml/min) from room temperature and kept isothermal for 10 min. It
94 was then heated from 50 to 1200 °C at a constant heating rate of 20 K/min in the presence of
95 pure CO₂ (40 ml/min). Prior to each test, the sample was further manually grounded to

96 smaller than 90 microns to minimize diffusion effects. About 5 mg of sample (accuracy up to
97 0.01 mg via PerkinElmer AD 6 autobalance) was loaded into a ceramic crucible for each test.
98 This slow heating rate and small amount of sample used would minimise mass transfer effects
99 and eliminate the heat transfer limitations in the CO₂ gasification process. Each test was
100 repeated three times to minimize the experimental error.

101 **2.4 Interactions indexes**

102 Thermal characteristics of coal, waste carbonaceous materials and their blends in CO₂
103 atmosphere were extracted from the TG/DTG profiles. The theoretical TG/DTG curves of the
104 blends were calculated by Eq. (1) based on the mass loss rates of each individual sample
105 assuming additive property applies. The deviation between experimental and calculated
106 curves was used to show the degree of interactions between samples [19, 20]:

$$107 \quad \frac{dm}{dt} = x_{SP1} \left(\frac{dm}{dt} \right)_{SP1} + x_{SP2} \left(\frac{dm}{dt} \right)_{SP2} \quad (1)$$

108 where $\left(\frac{dm}{dt} \right)_{SP1}$ and $\left(\frac{dm}{dt} \right)_{SP2}$ are the mass loss rates (%/min) of individual samples while
109 x_{SP1} and x_{SP2} are the corresponding mass fractions in the blends, respectively. The Root
110 Mean Square Interactions Index (RMSII) was applied to quantify the interactions between
111 components in the blend which compares the deviation of calculated value with experimental
112 value. Normally, a higher value of RMSII indicates a larger interaction taking place in the
113 process. The RMSII can be calculated using the Eq. (2) [21].

$$114 \quad RMSII = \sqrt{\frac{\sum_{i=1}^N \left(\frac{(dm/dt)_{EXP}^i - (dm/dt)_{CAL}^i}{(dm/dt)_{CAL}^i} \right)^2}{N}} \quad (2)$$

115 where $(dm/dt)_{EXP}$ and $(dm/dt)_{CAL}$ denote experimental and calculated mass loss rates values,
 116 respectively. N represents the number of points undertaken.

117 **3 Results and discussion**

118 **3.1 Properties of the samples**

119 Table 1 shows proximate, ultimate and ash analysis results of the samples studied in present
 120 work. For the proximate analysis, the relative standard deviation was ± 3 wt%, while for
 121 ultimate analysis, it was ± 2 wt%. As can be seen, volatile content and oxygen content varied
 122 significantly. Among all the tested samples, NMPCBs had the highest percentage of ash,
 123 which is mainly due to the presence of glass fiber. Hence, it would have some influence on
 124 gasification process. It is clear that tyre showed very similar properties in term of proximate
 125 and ultimate analysis data as coal. Its heating value is also very close to that of coal. Therefore,
 126 it is expected that the co-gasification of tyre with coal would have very little influence on the
 127 overall gasification process. On the other hand, negligible amount of ash was detected in
 128 polystyrene, which was completely decomposed, resulting in no fixed carbon formed after
 129 pyrolysis. Besides, polystyrene contained no sulphur and low percentage of nitrogen
 130 compared with the other samples.

131 Higher heating value (HHV) of individual samples were also included in Table 1 with relative
 132 standard deviation controlled within $\pm 4.5\%$. It is clear that polystyrene (41.7 MJ/kg, daf)
 133 exhibited the highest heating value, greater than that of coal (35.5 MJ/kg, daf). Meanwhile,
 134 the heating values of tyre (33.2 MJ/kg, daf) and NMPCBs (31.5 MJ/kg, daf) were all slightly
 135 lower than coal. Hence, blend with polystyrene, tyre or NMPCBs might not have a negative
 136 impact on co-gasification process. In contrast, oat straw (19.5 MJ/kg, daf) had the lowest
 137 heating value, which subsequently would result in a lower gasification temperature. As
 138 moderate low gasification temperature is one of the desired properties of the fuel, thus, it
 139 would enhance gasification performance in co-gasification process.

140 **Table 1: Proximate, ultimate analyses and calorific values of the samples.**

	AC	OS	NMPCBs	Tyre	PS
HHV (MJ/kg dry ash free)	35.5	19.5	31.5	33.2	41.7
Proximate analysis (wt %)					
Moisture	0.7	4.2	0.8	0.4	0.9
Volatile matter	34.6	70.7	25.1	62.9	99.1
Fixed carbon	48.2	18.2	6.9	19.6	-
Ash	16.5	6.9	67.2	17.1	-
Ultimate analysis ^{a,b} (wt %)					
C	81.3	37.4	39.8	80.9	92.1
H	4.9	5.3	3.6	6.4	7.7
O ^c	9.7	47.9	55.7	10.7	-
N	1.9	2.3	0.6	0.5	0.2
S	2.2	0.2	0.3	1.5	-
Ash composition (wt %, standard deviation $\pm 5\%$)					

SiO ₂	42.6	43.3	29.7	38.5	-
SO ₃	1.4	3.4	-	6.2	-
CaO	4.2	10.6	5.3	3.5	-
Na ₂ O	2.3	2.6	1.4	2.7	-
Fe ₂ O ₃	7.4	0.9	4.6	45.1	-
MgO	2.2	4.2	-	0.7	-
Al ₂ O ₃	39.1	2.2	5.3	2.4	-
K ₂ O	0.8	32.8	-	0.9	-
CuO	-	-	38.4	-	-
ZnO	-	-	5.7	-	-
Ni ₂ O ₃	-	-	9.6	-	-

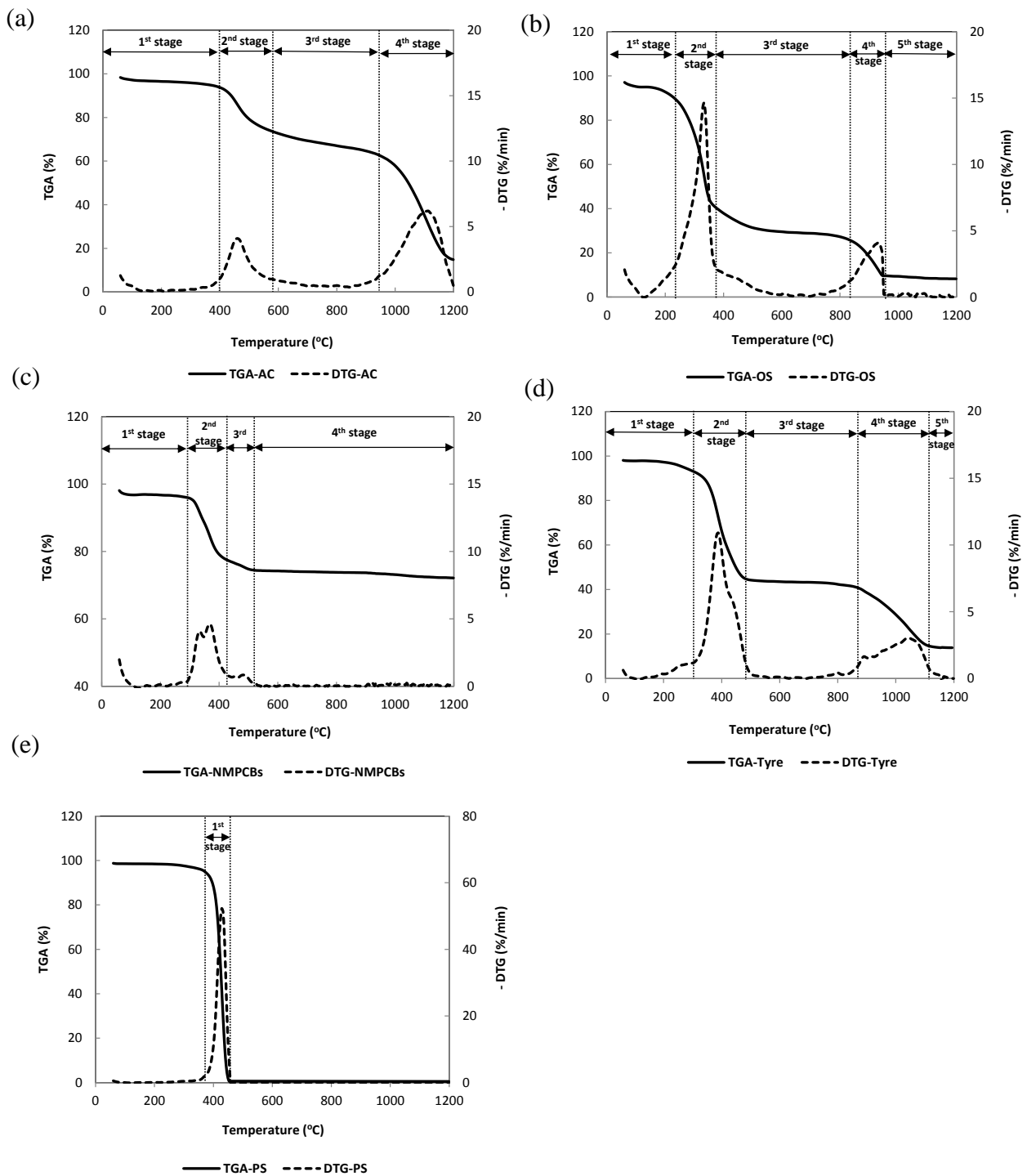
^aDry basis. ^bAsh free basis. ^cBy difference.

141 3.2 Thermal behaviours of the individual samples

142 Fig. 1 shows the TGA and DTG curves of coal and different waste carbonaceous materials
143 under CO₂ gasification. In this study, the instrument was calibrated to ensure that the
144 precision of ≤0.2% in TGA analysis was achieved. In Fig. 1, it is apparent that the gasification
145 processes involved a multi-stage thermal degradation where the number of stages and the
146 unique features of individual stage varied. The main mass losses in coal gasification took
147 place at 400-570 °C and 935-1190 °C, respectively (Fig. 1a). The first mass loss was due to
148 the release of volatiles while char gasification and thermal decomposition of minerals
149 contributed to the second mass loss. As expected in CO₂ gasification, the heterogeneous
150 reaction between coal char and CO₂ was much slower compared with combustion process.
151 This is because CO₂ is a weak oxidizing agent and the CO₂ gasification via Boudouard
152 reaction (C (S) + CO₂ → 2CO) is slow [22, 23]. Normally, at atmospheric pressure, the

153 Boudouard reaction is thermodynamically favourable at temperatures above 900 °C (initiated
154 at 800 °C) while the combustion of char can occur at significantly lower temperatures (below
155 630 °C). Two stages of mass losses were observed in oat straw as seen in Fig. 1b. The first
156 loss (240-375 °C) was attributed to the complete decomposition of hemi-cellulose and
157 cellulose and the partial decomposition of lignin [20, 24, 25]. The decomposition of
158 remaining lignin, char gasification and minerals decomposition contributed to the second
159 mass loss (820-950 °C). Unlike coal, CO₂ gasification of char derived from oat straw took
160 place at a lower temperature range. In general, biomass has a higher amount of volatiles
161 which generate a highly porous char compared with char derived from coal [26]. The porous
162 structure of char facilitates CO₂ diffusion, which leads to a better gasification performance.
163 The gasification of oat straw therefore completed at lower temperatures. It was reported that
164 the reactivity of biomass char is usually higher than the chars produced from coal [27, 28].
165 This implies that compared with coal char, biomass char can be gasified at much lower
166 temperature which is the case for oat straw.

167 Fig. 1c shows the main mass loss experienced by NMPCBs in the second stage which is
168 illustrated at temperature from 295 to 410 °C. In spite of NMPCBs having the lowest
169 volatiles, its maximum mass loss was occurred at low temperature region.



170

171 **Figure 1: CO₂ gasification distribution of the TGA and DTG curves of (a) coal, (b) oat straw, (c)**

172

NMPCBs, (d) tyre and (e) polystyrene.

173 Typically, epoxy resin is the major component of the NMPCBs which is mixed with

174 brominated compounds [29, 30]. The decomposition of epoxy resin, degradable part of

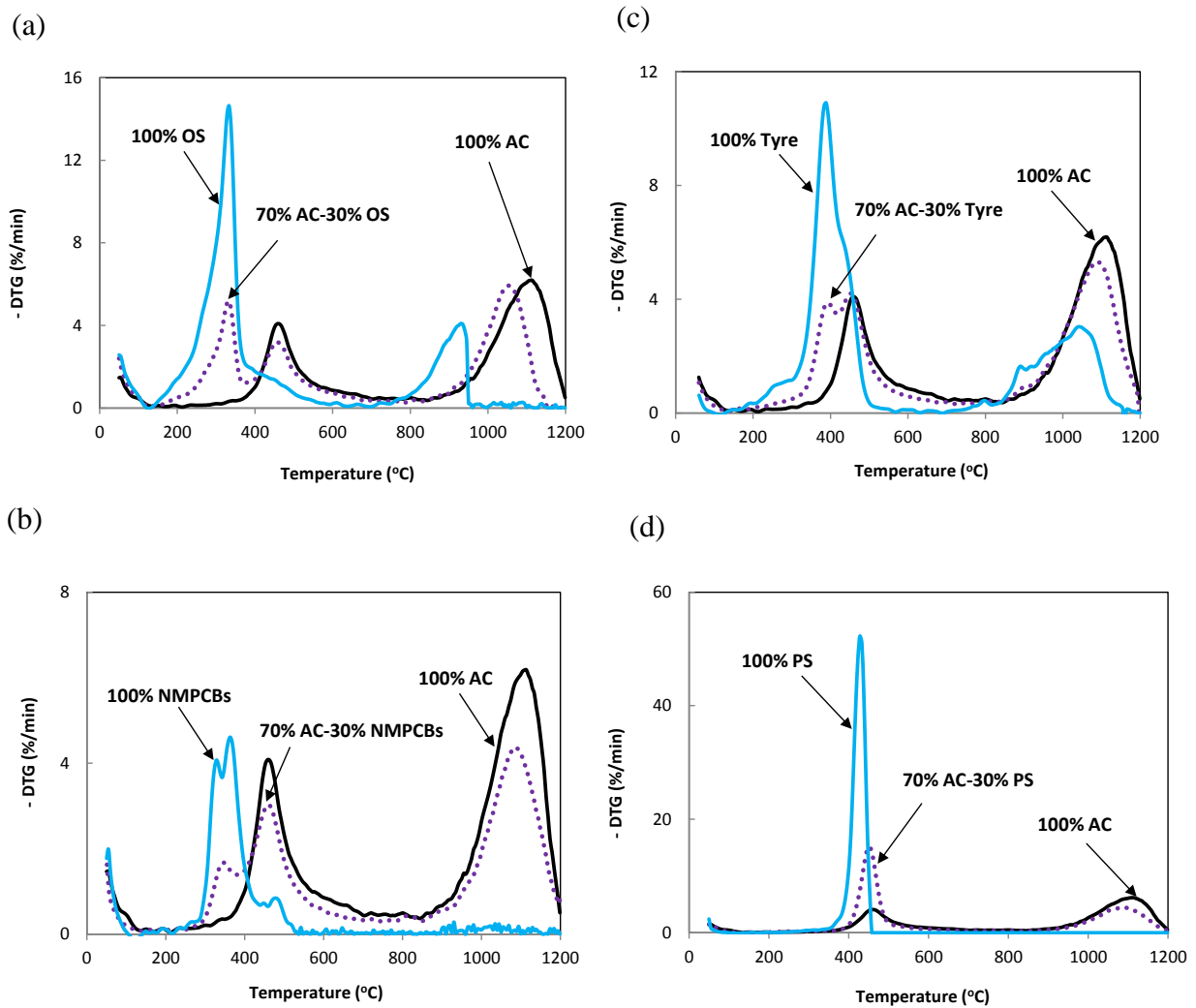
175 NMPCBs, started at around 300 °C. Consequently, thermal decomposition of NMPCBs

176 consists of two stages, the decomposition of brominated compounds and decomposition of
177 non-brominated compounds. The possible reason for the existence of small peak before the
178 main peak was the partial overlapping of these two reactions [30]. As seen in Fig. 1c, a
179 smaller DTG peak which was situated between the temperatures of 465 to 510 °C, denoted the
180 second main mass loss due to the release of volatiles due to the decomposition of brominated
181 compounds in NMPCBs. It is important to notice that the value of this mass loss rate was
182 smaller (0.85 wt%/min) in comparison with mass loss rates noticed in other samples. As seen
183 in Fig. 1d, tyre also exhibited the first mass loss at low temperature region (300-490 °C)
184 similar to NMPCBs while the second mass loss happened at relatively high temperature
185 region (875-1110 °C). Generally, tyre contains small portion of additives (less than 30 wt%)
186 and the rest is rubber (natural and synthetic) [31, 32]. The first mass loss was caused by the
187 decomposition of the additives and both types of rubber which occurred at lower temperature.
188 Afterwards, the second mass loss depicted CO₂ char gasification. Higher percentage of carbon
189 in tyre might be the reason for this slow gasification reaction. On the other hand, polystyrene
190 experienced a single stage degradation at a higher temperature region (350-455 °C) compared
191 with other waste carbonaceous materials. From Fig. 1e, it can be seen that polystyrene had a
192 negligible mass loss up to 250 °C, whereas a slight mass loss was detected at temperature
193 between 250 to 350 °C. This confirmed that polystyrene was thermally stable up to 350 °C.
194 Degradation completed at 455 °C and during this stage the mass loss observed was 98.5 wt%
195 due to the thermal cracking of light organics and other carbonaceous heavy organics to low

196 molecular weight compounds. The overall mechanism is believed to be dictated by the
197 combination of end-chain initiation, depolymerisation, intramolecular hydrogen transfer, and
198 bimolecular termination processes. The changes in mass loss are caused by inter-molecular
199 transfer reactions while devolatilisation is governed by intramolecular transfer reactions.
200 Above 455 °C, no residue was observed, which confirmed the complete degradation of
201 polystyrene in CO₂ gasification. In general, gasification characteristics such as initial
202 decomposition temperature and final mass loss temperature are the crucial parameters of the
203 fuel performance. As can be seen in Fig. 1, oat straw had the lowest initial decomposition
204 temperature (281 °C). In contrast, coal and polystyrene experienced the two highest initial
205 decomposition temperatures (415 and 407 °C). However, the final maximum mass loss
206 temperatures was in the order of polystyrene (428 °C), NMPCBs (479 °C) and oat straw (931
207 °C), respectively which suggested that polystyrene and NMPCBs were more reactive
208 compared with oat straw. Moreover, the highest maximum mass loss rate (49.7 wt%/min) and
209 the lowest gasification time (18.9 min) were observed for polystyrene. Therefore, the use of
210 polystyrene as a fuel for co-gasification application would be more beneficial.

211 **3.3 Co-gasification characteristics of coal and carbonaceous materials**

212 Fig. 2 describes the co-gasification behaviours of coal and carbonaceous materials and the
213 characteristics of individual samples and blends are listed in Table 2.



214

215

Figure 2: CO₂ gasification distributions of (a) coal/oat straw, (b) coal/NMPCBs, (c) coal/tyre and (d)

216

coal/polystyrene blends (standard deviation $\pm 1.3\%$).

217

In general, curves of the blends were found in the location between those of the original

218

samples. From Fig. 2a, it is clear that coal/oat straw blends had three-stage mass loss rather

219

than the two-stage mass loss identified for the original oat straw sample. In the case of blends,

220

the first mass loss was mainly due to the volatiles release from decomposition of

221

hemicellulose and cellulose in oat straw whereas the third one was mostly caused by char

222

gasification. Commonly, the initial devolatilisation temperature of coal is approximately the

223

same as the terminal devolatilisation temperature of biomass. Therefore, the second mass loss

224 was attributed mainly to the devolatilisation of coal, while the gasification of chars derived
225 from both oat straw and coal collectively resulted in the third mass loss. As shown in Table 2,
226 the coal (415 °C) started to devolatilise at a higher temperature than that of the oat straw (281
227 °C). In addition, the maximum mass loss temperatures of coal and oat straw were 458/1108
228 °C and 332/931 °C, respectively. It is interesting to see that the first and the second mass loss
229 temperatures of the blends did not vary significantly. However, the change of the third mass
230 loss temperatures was noticed. This indicated that the blending of oat straw with coal did not
231 have significant influence on the devolatilisation stage but affected the char gasification
232 process. Besides, as oat straw percentage in blend increased, the reduction in the initial
233 decomposition temperature (T_i) of the blends was also observed, which contributed to a lower
234 devolatilisation temperature in co-gasification process. The experimental results also
235 demonstrated that the addition of oat straw shifted the CO₂ gasification process to a low
236 temperature region by reducing the overall maximum mass loss temperatures (T_{max}). The
237 higher volatiles content in oat straw (shown in Table 1) was the reason for these phenomena
238 as oat straw burns at a much lower temperature compared with coal. Besides, DTG value of
239 the first mass loss increased (1.9 wt%/min to 5.2 wt%/min due to increment of blending
240 proportion from 10% to 30%) due to higher volatiles content while it decreased (6 wt%/min
241 to 5.9 wt%/min) in the third mass loss due to increasing amount of the char derived from coal.
242

Table 2: CO₂ gasification characteristic parameters of blends and individual samples.

Sample	T_i	T_{max} (°C)	t_{max} (min)	DTG_{max} (%/min)
Australian coal	415	458/1108	20.5/52.8	4.1/6.1
Blend 1 (10% oat straw)	301	335/460/1091	14.2/20.5/52.2	1.9/3.9/6
Blend 2 (30% oat straw)	294	333/456/1053	14.1/20.3/50.1	5.2/3.2/5.9
Oat straw	281	332/931	14.1/44.2	14.7/4.1
Blend 1 (10% NMPCBs)	407	456/1100	20.6/53.2	3.8/5.9
Blend 2 (30% NMPCBs)	353	344/453/1082	14.7/20.5/51.7	1.7/3.0/4.3
NMPCBs	305	364/479	15.7/21.5	4.5/0.9
Blend 1 (10% tyre)	400	457/1106	20.5/52.7	4.2/5.9
Blend 2 (30% tyre)	365	395/458/1088	17.3/20.3/51.8	3.9/4.2/5.3
Tyre	357	394/1046	17.2/50.1	10.4/3
Blend 1 (10% PS)	412	456/1104	20.2/52.5	7.3/5.6
Blend 2 (30% PS)	410	453/1082	20/51.8	15.1/4.5
Polystyrene (PS)	407	428	18.9	49.7

244 T_i =Initial decomposition temperature, T_{max} = Maximum mass loss temperature, t_{max} =maximum
 245 reaction time and DTG_{max} = Maximum mass loss rate.

246 Uncertainty of temperature: $\pm 1^\circ\text{C}$. Uncertainty of DTG_{max} : ± 0.15 %/min.

247 When NMPCBs was gasified with coal at the high blending ratio, the gasification process
 248 featured three main mass loss stages as seen in Fig. 2b. The first mass loss stage occurred at
 249 temperature between 330 and 380 °C where the decomposition of NMPCBs took place. The
 250 second DTG_{max} (400-485 °C) indicated the release of volatiles from both coal and NMPCBs
 251 whereas the third DTG_{max} depicted the stage of CO₂ gasification of NMPCBs and coal
 252 derived chars. In contrast, at low blending ratios, such as 10 wt% NMPCBs, only two main
 253 mass loss stages were noticed at similar temperature ranges as coal in co-gasification. Here,
 254 the value of first DTG_{max} (Table 2) decreased because of the lower amount of volatiles in the

255 blend contributed by NMPCBs. Meanwhile, the decrement of the second DTG_{max} was as a
256 result of the lower amount of NMPCBs char. From Table 2, it is clear that the initial
257 devolatilisation temperature and the first DTG_{max} temperature of the blend were shifted to a
258 lower temperature region as the proportion of NMPCBs increased while the final DTG_{max}
259 temperature was also shifted to a lower temperature due to the reduced amount of coal derived
260 char. Therefore, it can be concluded that the co-gasification of coal and NMPCBs completed
261 at a relatively lower temperature despite of a slight reduction of the maximum mass loss rate.

262 For coal/tyre blends as presented in Fig. 2c, two-stage mass loss was noticed at the low
263 blending ratio. The results on gasification parameters listed in Table 2 demonstrated that coal
264 had a dominant effect on the blend of 10 wt% tyre since it showed similar behaviours with the
265 characteristics of coal. It's mainly because coal and tyre have similar physical and chemical
266 properties as shown in Table 1. These properties were assumed as a result of the narrow
267 difference of initial decomposition temperatures between coal (415 °C) and tyre (357 °C), and
268 also a very small amount of tyre being blended. In contrast, the blend of 30 wt% tyre
269 experienced three-stage mass loss. From Table 2, it can be found that the first and the second
270 mass loss of the blend occurred at the same temperature as the first mass loss of original tyre
271 and coal, respectively. This means that the decomposition of tyre and coal in the blend was
272 took place sequentially rather than simultaneously. However, it can be seen from Fig. 2c that
273 gasification was shifted toward lower temperature with the increase of tyre fraction in the

274 blends. The reason behind the shifting was because of the thermal properties of tyre which
275 decomposes relatively lower temperature than coal. Besides, the third mass loss rate which
276 represented the char gasification of both coal and tyre was reduced (about 10% because of
277 increment of blending proportion from 10% to 30%) due to the low amount of char generated
278 from coal in the blend.

279 Among all the blend samples investigated in this study, coal/polystyrene blends exhibited
280 different behaviours as illustrated in Fig. 2d. As polystyrene decomposed through a single-
281 stage mass loss without any solid residue and its initial decomposition took place at a slightly
282 slower temperature than coal, a complete coincidence between whole polystyrene mass loss
283 and first mass loss of coal was observed. Hence, devolatilisation stage of the blend samples
284 was represented by a single peak in DTG profile. Compared with coal, polystyrene contained
285 approximately three times higher amount of volatiles, which resulted in the substantial
286 increment of the first mass loss rates in blends. Similar to other blends, a gradual decrement
287 of the second mass loss rate was observed when polystyrene was blended with coal. At the
288 same time, the temperature corresponding to the maximum mass loss was also reduced. This
289 was affected by the combination of the decrease in the percentage of coal and the increment
290 of volatiles from polystyrene in the blends.

291 **3.4 Interactions between coal and carbonaceous materials**

292 To further understand the interactions in blend, the experimental and calculated DTG curves
293 of the blends under CO₂ atmosphere are compared in Fig. 3. Overall, the curves illustrate that
294 the interactions existed as the experimental curves of blends deviated from the calculated
295 curves for the same blends [19, 20]. However, the deviation was not consistent at different
296 stages of the entire process and varied with the blending of different materials, blending ratio
297 and temperature range. From Fig. 3a, deviations were observed for coal/oat straw blends at
298 two different temperature regions. This indicated the existence of significant interactions in
299 the range of 950-1200 °C and weaker interactions between 390-700 °C for both high and low
300 blending ratios. Similarly, as seen in Fig. 3d, coal/polystyrene blends also showed significant
301 interactions at different temperature ranges of 400-500 °C and 1000-1200 °C. For
302 coal/NMPCBs blends (Fig. 3b), analogous behaviours were noticed where stronger and
303 weaker interactions occurred in the temperatures ranges of 1050-1200 °C and 600-900 °C,
304 respectively. Correspondingly, Fig. 3c depicted that in temperature range of 1160-1200 °C,
305 coal/tyre blends experienced noticeable interactions while insignificant interactions occurred
306 from 400 to 600 °C.

307 In order to determine the intensity of the interactions in the whole process, the root mean
308 square interactions index (RMSII) of the blends (as detailed in Eq. 2) were also evaluated and
309 listed in Table 3, which is of an accumulated uncertainty of ± 0.01 . Overall, the presence of

310 interactions was evident in the blends as demonstrated by RMSII value. From Table 3, it is
311 apparent that the higher the amount of carbonaceous material was added into the blend, the
312 higher the value of RMSII was observed. Moreover, regardless of blending ratio, RMSII
313 values of char gasification stage were higher than those of devolatilisation stage, except for
314 polystyrene, which ratified the strong interactions during char gasification stage. However,
315 significant interactions were noticed in devolatilisation stage for coal/polystyrene blends as
316 demonstrated by high RMSII value. At both blending ratios, the highest RMSII values in
317 devolatilisation and char gasification stages were exhibited by coal/polystyrene blends and
318 coal/oat straw blends, respectively. It is important to point out that the interactions in char
319 gasification stage of coal/NMPCBs blend at high blending ratio were considerably lower than
320 those of other ash containing blends. As seen in Table 1, NMPCBs had the highest ash
321 content (67.2 wt%) among all the carbonaceous materials studied. Thus, the high ash content
322 of NMPCBs which subsequently result in ash inhibition effect contributing to its weakest
323 interactions [33].

324 Table 4 shows the comparison of RMSII values between co-pyrolysis and CO₂ co-gasification
325 processes which were conducted under the same temperature but different atmosphere. From
326 Table 4, it is apparent that coal/oat straw blend showed higher interactions during gasification
327 process as demonstrated by its RMSII value which was over two times higher than that of

328 pyrolysis process. The reasons behind the aforementioned characteristics can be well
329 explained as follows.

330 It was observed that DTG curves for the devolatilisation stage in pyrolysis were similar to
331 those in CO₂ gasification so that the main DTG_{max} was almost coincided each other at the
332 same temperature. With the increase of temperature (above 900 °C), considerable additional
333 weight loss was noticed in CO₂ gasification process. This was because of the reaction of CO₂
334 with the remaining char (mostly) (Eq. 3) as CO₂ has reaction activity at high temperature
335 condition [34, 35]. Thus, it is confirmed that char gasification process played a key role for
336 these interactions.



338 Similarly, enhanced interactions were noticed for the blends of coal with each NMPCB and
339 tyre in CO₂ co-gasification. However, the enhancements in these blends were considerably
340 lower than that of coal/oat straw blend. This was due to the fact that char derived from
341 biomass are normally more reactive compared with those derived from other carbonaceous
342 materials such as NMPCBs. Furthermore, this phenomenon might be originated from mineral
343 content in these samples which will be discussed in the following section. Exceptionally,
344 coal/polystyrene blend had a slightly lower RMSII value in CO₂ gasification process which
345 revealed weaker interactions than in its pyrolysis process. This indicated the influence of CO₂
346 in polystyrene devolatilisation process as the contribution of C + CO₂ reaction is extremely

347 small since char content was literally zero. It is reported that the devolatilisation of
 348 polystyrene mainly occurred because of the breaking of C-C and C-H bonds [36]. During CO₂
 349 gasification, CO₂ reacts randomly with these bonds [34]. Hence, coal/polystyrene blend is
 350 likely to demonstrate less interaction in this process as also presented in Table 4. Thus, it can
 351 be summarised that char gasification process increased the interactions on blends of oat straw,
 352 NMPCBs and tyre with coal while the devolatilisation process had a significant role on
 353 coal/polystyrene blend. Nonetheless, it is interesting to note that coal/polystyrene blend
 354 revealed the highest interactions in both processes as shown by its highest RMSII values
 355 compared to the other blends. This was due to the high volatiles content in polystyrene sample
 356 which will be detailed in section 3.5.

357 The aforementioned discussion has suggested that the mechanism of interactions between coal
 358 and carbonaceous materials were highly influenced by the properties and percentage of
 359 carbonaceous materials being added into the blends. Furthermore, the effect of CO₂ as
 360 gasification agent on interactions was also noticed.

361 **Table 3: RMSII value of experimental and calculated DTG curves.**

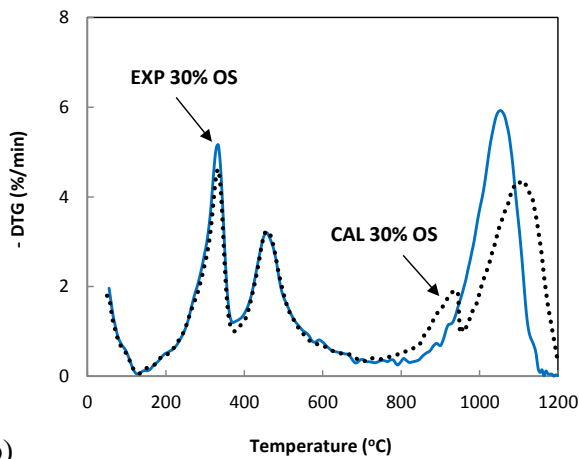
Carbonaceous materials	RMSII (SD±0.01)			
	Devolatilisation		Char gasification	
	10%	30%	10%	30%
Oat straw	0.10	0.09	0.26	0.71
NMPCBs	0.13	0.25	0.20	0.24
Tyre	0.06	0.10	0.18	0.60
Polystyrene	0.32	0.92	0.13	0.17

362 **Table 4: Comparison of RMSII values between co-gasification and co-pyrolysis processes (70:30 blends).**

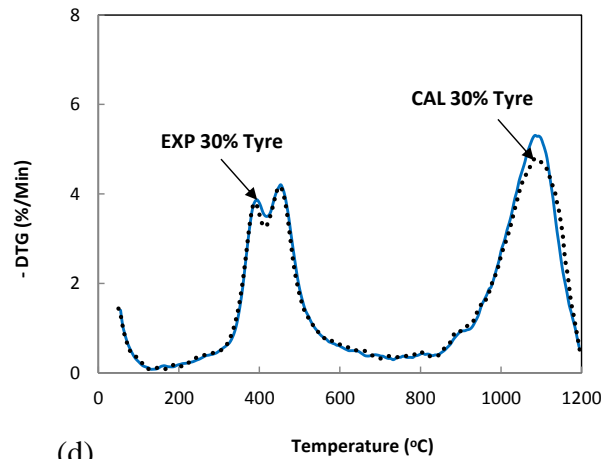
Blends	CO ₂ co-gasification	Co-pyrolysis
AC/OS	0.43	0.20
AC/NMPCBs	0.25	0.22
AC/tyre	0.29	0.25
AC/PS	0.56	0.60

363

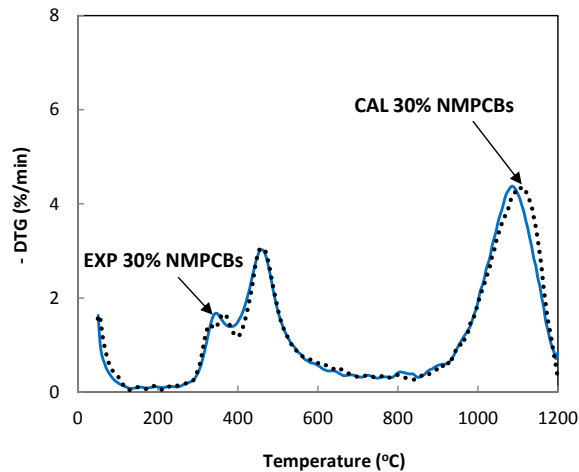
364 (a)



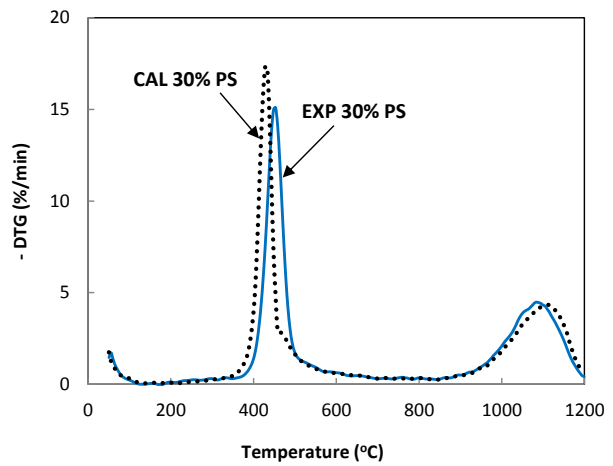
(c)



(b)



(d)



365

366 **Figure 3: Comparison of experimental and calculated DTG curves of (a) coal/oat straw, (b) coal/NMPCBs,**
 367 **(c) coal/tyre and (d) coal/polystyrene blends.**

368 **3.5 Mechanism of interactions**

369 In spite of blending equal proportions of different carbonaceous materials with coal, intensity
 370 and temperature at which interactions took place varied considerably. High level of volatile

371 content and high reactivity of carbonaceous materials were the reasons for the existence of
372 interactions in the blends [19, 37]. As previously explained, at both low and high blending
373 ratios, coal/polystyrene blends exhibited the highest interactions during devolatilisation stage.
374 This was due to the generation of large amount of reactive free radicals from polystyrene
375 cracking of as a result of containing a relatively higher amount of volatiles. The free radicals
376 were released through thermal decomposition of polystyrene, which react with coal and
377 enhance the devolatilisation and coal char gasification. In addition, the volatiles generated by
378 coal can react with the gases resulted from the cracking of the heavy volatiles as well as light
379 molecules (mostly hydrocarbon) derived from polystyrene. Therefore, a sluggish increment of
380 the secondary char generation is observed because of the inhibition of reverse Boudouard
381 reaction. Furthermore, the maximum weight loss rate also influences the generation of
382 different kinds of radicals. The rate of radicals formation is increased by their stability; hence
383 the conversion rate is greater when more stable radicals formed during devolatilisation
384 process [38]. Applying this concept to carbonaceous materials, the maximum weight loss rate
385 obtained by polystyrene is very high and this suggests the generation of stable radicals. This
386 phenomenon also assisted to the significant interactions during devolatilisation stage. On the
387 other side, even though NMPCBs had lower amount of volatiles, stronger interactions were
388 observed at devolatilisation stage. This behaviour was due to epoxy resin, a main part of
389 NMPCBs, which decomposed at relatively low temperature because of its high reactivity.

390 The interactions can also be caused by the catalytic effect of alkali and alkaline earth metals
391 (AAEM) contained in ash of the original samples [37, 39, 40]. It is reported that AAEM,
392 particularly, Ca and K species are active catalyst for gasification process [41, 42].

393 In the beginning of decomposition process, calcium, potassium and the other AAEM species
394 are combined with the carboxyl and phenolic groups, forming organic molecules in coal or
395 carbonaceous sample [43]. At the same time, the organic substances in the solid surface are
396 transformed to a micro-crystalline char, favouring the structure of char to become more
397 porous which enhances the reactivity in gasification [42].

398 Afterwards, this porous char adsorbs the AAEM onto its surface during the volatile-char
399 interactions stage [44]. Moreover, the presence of intermediate alkali-surface compounds
400 creates a bigger gap between AAEM and carbon which result in significant volume
401 expansion. These behaviours therefore contribute to the promotion of the gasification reaction
402 through weakening the carbon-carbon bonds present between layers [41].

403 As seen in Table 1, oat straw ash has demonstrated mostly the highest amount of these AAEM
404 among the others. In particular, CaO and K₂O in oat straw were found to be 10.6 wt% and
405 32.8 wt%, respectively, which were essential components for catalytic effect. Therefore, these
406 mainly contributed to the highest interactions in char gasification stage shown by coal/oat
407 straw blends compared with other blends. Meanwhile, the ash from NMPCBs, tyre and coal
408 samples contain a comparable percentage of AAEM, much lower than those of oat straw.

409 Moreover, ash compositional data showed that oat straw had high silica content which has
410 been demonstrated to reduce the reactivity of char [45]. However, the proportion of silica in
411 the other samples were relatively similar to each other, thus, the overall effect from silica was
412 assumed to be similar regardless of types of samples. Similarly, alumina also acts as a
413 deactivator for the catalytic effect [46]. As the lowest percentage of Al_2O_3 (2.2 wt%) was
414 observed in oat straw ash, so that oat straw had the least obstacle to undergo the catalytic
415 activities. It is worth noting that coal/tyre blend exhibited higher interactions than NMPCBs at
416 high blending ratio despite both had almost equal percentage of AAEM. The reason behind
417 these characteristics can be explained by Fe_2O_3 in the ash. Previous study revealed that metal
418 oxide such as Fe_2O_3 increased the gasification activity of coal due to the catalytic effect in
419 CO_2 gasification [47]. As tyre ash contain higher percentage of Fe_2O_3 (45.1 wt%), hence, it
420 could act as a catalyst for char- CO_2 reaction.

421 **4 Conclusion**

422 CO_2 co-gasification of coal with four different waste carbonaceous materials was investigated
423 in a thermogravimetric analyser. The influence of waste origin on the mechanism of
424 interactions was also discussed. The main findings are summarised as follows: (i) significant
425 high volatiles content of carbonaceous materials could plays a vital role in enhancing the
426 degree of interactions during devolatilisation stage; (ii) AAEM metals content such as CaO
427 and K_2O had a key influence on strong interactions in char gasification stage due to their

428 catalytic effect; (iii) the improvement of coal gasification performance is noticed as
429 demonstrated by its gasification characteristics such as initial decomposition temperature and
430 final mass loss temperature with the addition of carbonaceous materials, irrespective of stage
431 at which the interactions occurred. The best performances of gasification process in CO₂
432 atmosphere were achieved by using polystyrene and oat straw as carbonaceous materials to be
433 blended with coal. These phenomena were as expected mainly due to polystyrene having the
434 highest volatiles content whereas oat straw presented the catalytic effect from its AAEM
435 metals. Furthermore, the comparison between co-pyrolysis and CO₂ gasification processes by
436 using RMSII values confirmed the influence of CO₂ as a gasifying agent on the presence of
437 interactions in the blends. Hence, these experimental findings have confirmed that CO₂
438 gasification of coal can be considerably improved by adding polystyrene and oat straw into
439 the process.

440 **Acknowledgement**

441 Following funding bodies are acknowledged for partially sponsored this piece research:
442 Ningbo Bureau of Science and Technology (Innovation Team Scheme, 2012B82011, and
443 Major Research Scheme, 2012B10042), and Department of Science and Technology Zhejiang
444 (Provincial Innovation Team on SO_x and NO_x Removal Technologies, 2011R50017). The
445 University of Nottingham Ningbo China is acknowledged for providing full scholarship to the
446 first author.

447 5 References

448

449

- 450 1. Wu, T., et al., *Characteristics and synergistic effects of co-firing of coal and*
451 *carbonaceous wastes*. Fuel, 2013. **104**(0): p. 194-200.
- 452 2. Sami, M., K. Annamalai, and M. Wooldridge, *Co-firing of coal and biomass fuel*
453 *blends*. Progress in Energy and Combustion Science, 2001. **27**(2): p. 171-214.
- 454 3. Pan, Y.G., et al., *Fluidized-bed co-gasification of residual biomass/poor coal blends*
455 *for fuel gas production*. Fuel, 2000. **79**(11): p. 1317-1326.
- 456 4. Seo, M.W., et al., *Gasification characteristics of coal/biomass blend in a dual*
457 *circulating fluidized bed reactor*. Energy & Fuels, 2010. **24**(5): p. 3108-3118.
- 458 5. Wang, L., et al., *CO₂ Gasification of Chars Prepared from Wood and Forest Residue:*
459 *A Kinetic Study*. Energy & Fuels, 2013. **27**(10): p. 6098-6107.
- 460 6. Skodras, G., G. Nenes, and N. Zafeiriou, *Low rank coal – CO₂ gasification:*
461 *Experimental study, analysis of the kinetic parameters by Weibull distribution and*
462 *compensation effect*. Applied Thermal Engineering, 2015. **74**(0): p. 111-118.
- 463 7. Lahijani, P., et al., *CO₂ gasification reactivity of biomass char: Catalytic influence of*
464 *alkali, alkaline earth and transition metal salts*. Bioresource Technology, 2013.
465 **144**(0): p. 288-295.
- 466 8. Butterman HC, C.M., *CO₂ as a Carbon Neutral Fuel Source via Enhanced Biomass*
467 *Gasification*. Environ. Sci. Technol., 2009(43): p. 9030–9037.
- 468 9. Edreis, E.M.A., G. Luo, and H. Yao, *Investigations of the structure and thermal*
469 *kinetic analysis of sugarcane bagasse char during non-isothermal CO₂ gasification*.
470 Journal of Analytical and Applied Pyrolysis, 2014. **107**(0): p. 107-115.
- 471 10. Kirtania, K., et al., *Comparison of CO₂ and steam gasification reactivity of algal and*
472 *woody biomass chars*. Fuel Processing Technology, 2014. **117**(0): p. 44-52.
- 473 11. Khalil, R., et al., *CO₂ gasification of biomass chars: a kinetic study*. Energy & Fuels,
474 2008. **23**(1): p. 94-100.
- 475 12. Sircar, I., et al., *Experimental and modeling study of pinewood char gasification with*
476 *CO₂*. Fuel, 2014. **119**(0): p. 38-46.
- 477 13. Lewis, A.D., E.G. Fletcher, and T.H. Fletcher, *Pyrolysis and CO₂ Gasification Rates*
478 *of Biomass at High Heating Rate Conditions*. 2013.
- 479 14. Huo, W., et al., *Study on CO₂ gasification reactivity and physical characteristics of*
480 *biomass, petroleum coke and coal chars*. Bioresource Technology, 2014. **159**(0): p.
481 143-149.
- 482 15. Pohořelý, M., et al., *CO₂ as moderator for biomass gasification*. Fuel, 2014. **117**, Part
483 **A**(0): p. 198-205.

- 484 16. Hanaoka, T., S. Hiasa, and Y. Edashige, *Syngas production by CO₂/O₂ gasification of*
485 *aquatic biomass*. *Fuel Processing Technology*, 2013. **116**(0): p. 9-15.
- 486 17. BS/EN15443:2011, *Solid recovered fuels. Methods for the preparation of the*
487 *laboratory sample*. 2011.
- 488 18. ISO17246:2010, *Coal - Proximate analysis*. 2010.
- 489 19. Edreis, E.M.A., et al., *Synergistic effects and kinetics thermal behaviour of petroleum*
490 *coke/biomass blends during H₂O co-gasification*. *Energy Conversion and*
491 *Management*, 2014. **79**(0): p. 355-366.
- 492 20. Gil, M.V., et al., *Thermal behaviour and kinetics of coal/biomass blends during co-*
493 *combustion*. *Bioresource Technology*, 2010. **101**(14): p. 5601-5608.
- 494 21. Wang, Q., et al., *Interactions and kinetic analysis of oil shale semi-coke with cornstalk*
495 *during co-combustion*. *Applied Energy*, 2011. **88**(6): p. 2080-2087.
- 496 22. Butterman, H.C. and M.J. Castaldi. *CO₂ enhanced steam gasification of biomass*
497 *fuels*. in *16th Annual North American Waste-to-Energy Conference*. 2008. American
498 Society of Mechanical Engineers.
- 499 23. Basu, P., *Combustion and gasification in fluidized beds*. 2006: CRC press.
- 500 24. Sahu, S.G., N. Chakraborty, and P. Sarkar, *Coal–biomass co-combustion: An*
501 *overview*. *Renewable and Sustainable Energy Reviews*, 2014. **39**(0): p. 575-586.
- 502 25. Xie, Z. and X. Ma, *The thermal behaviour of the co-combustion between paper sludge*
503 *and rice straw*. *Bioresource Technology*, 2013. **146**(0): p. 611-618.
- 504 26. Basu, P., *Biomass gasification and pyrolysis: practical design and theory*. 2010:
505 Academic press.
- 506 27. Backreedy, R.I., et al., *Modeling the reaction of oxygen with coal and biomass chars*.
507 *Proceedings of the Combustion Institute*, 2002. **29**(1): p. 415-421.
- 508 28. Wang, X., et al., *Kinetics investigation on the combustion of biochar in O₂/CO₂*
509 *atmosphere*. *Environmental Progress & Sustainable Energy*, 2015. **34**(3): p. 923-932.
- 510 29. Wu, W. and K. Qiu, *Vacuum co-pyrolysis of Chinese fir sawdust and waste printed*
511 *circuit boards. Part I: Influence of mass ratio of reactants*. *Journal of Analytical and*
512 *Applied Pyrolysis*, 2014. **105**(0): p. 252-261.
- 513 30. Quan, C., A. Li, and N. Gao, *Thermogravimetric analysis and kinetic study on large*
514 *particles of printed circuit board wastes*. *Waste Management*, 2009. **29**(8): p. 2353-
515 2360.
- 516 31. Martínez, J.D., et al., *Waste tyre pyrolysis – A review*. *Renewable and Sustainable*
517 *Energy Reviews*, 2013. **23**: p. 179-213.
- 518 32. Chen, F. and J. Qian, *Studies of the thermal degradation of waste rubber*. *Waste*
519 *Management*, 2003. **23**(6): p. 463-467.
- 520 33. Zhang, Y., et al., *Effect of fuel origin on synergy during co-gasification of biomass*
521 *and coal in CO₂*. *Bioresource Technology*, 2016. **200**: p. 789-794.

- 522 34. Chen, T., et al., *Key thermal events during pyrolysis and CO₂-gasification of selected*
523 *combustible solid wastes in a thermogravimetric analyser*. Fuel, 2014. **137**: p. 77-84.
- 524 35. Lai, Z., et al., *Thermogravimetric analysis of the thermal decomposition of MSW in*
525 *N₂, CO₂ and CO₂/N₂ atmospheres*. Fuel Processing Technology, 2012. **102**: p. 18-23.
- 526 36. Grammelis, P., et al., *Pyrolysis kinetics and combustion characteristics of waste*
527 *recovered fuels*. Fuel, 2009. **88**(1): p. 195-205.
- 528 37. Tchapda, A.H. and S.V. Pisupati, *A review of thermal co-conversion of coal and*
529 *biomass/waste*. Energies, 2014. **7**(3): p. 1098-1148.
- 530 38. Kiran, N., E. Ekinici, and C. Snape, *Recycling of plastic wastes via pyrolysis*.
531 *Resources, Conservation and Recycling*, 2000. **29**(4): p. 273-283.
- 532 39. Edreis, E.M.A., et al., *CO₂ co-gasification of lower sulphur petroleum coke and sugar*
533 *cane bagasse via TG-FTIR analysis technique*. Bioresource Technology, 2013.
534 **136**(0): p. 595-603.
- 535 40. Nemanova, V., et al., *Co-gasification of petroleum coke and biomass*. Fuel, 2014. **117**,
536 **Part A**(0): p. 870-875.
- 537 41. Huang, Y., et al., *Effects of metal catalysts on CO₂ gasification reactivity of biomass*
538 *char*. Biotechnology Advances, 2009. **27**(5): p. 568-572.
- 539 42. Mitsuoka, K., et al., *Gasification of woody biomass char with CO₂: The catalytic*
540 *effects of K and Ca species on char gasification reactivity*. Fuel Processing
541 *Technology*, 2011. **92**(1): p. 26-31.
- 542 43. Quyn, D.M., et al., *Volatilisation and catalytic effects of alkali and alkaline earth*
543 *metallic species during the pyrolysis and gasification of Victorian brown coal. Part*
544 *IV. Catalytic effects of NaCl and ion-exchangeable Na in coal on char reactivity*☆.
545 *Fuel*, 2003. **82**(5): p. 587-593.
- 546 44. Li, X. and C.-Z. Li, *Volatilisation and catalytic effects of alkali and alkaline earth*
547 *metallic species during the pyrolysis and gasification of Victorian brown coal. Part*
548 *VIII. Catalysis and changes in char structure during gasification in steam*. Fuel, 2006.
549 **85**(10-11): p. 1518-1525.
- 550 45. Kannan, M.P. and G.N. Richards, *Gasification of biomass chars in carbon dioxide:*
551 *dependence of gasification rate on the indigenous metal content*. Fuel, 1990. **69**(6): p.
552 747-753.
- 553 46. Kajita, M., et al., *Catalytic and Noncatalytic Mechanisms in Steam Gasification of*
554 *Char from the Pyrolysis of Biomass*†. Energy & Fuels, 2009. **24**(1): p. 108-116.
- 555 47. He, P., et al., *Simultaneous Low-Cost Carbon Sources and CO₂ Valorizations through*
556 *Catalytic Gasification*. Energy & Fuels, 2015. **29**(11): p. 7497-7507.
557
558